

Exploding stars show us that time slows down in the distant Universe!

~~The Dark Energy Survey Supernova Program: Slow supernovae show cosmological time dilation out to $z \sim 1$.~~

Ryan M. T. White^{1*}, Tamara M. Davis¹, Geraint F. Lewis², Christopher Lidman^{3,4}, Paul Shah⁵, T. M. C. Abbott⁶, M. Aguena⁷, S. Allam⁸, F. Andrade-Oliveira⁹, J. Asorey¹⁰, D. Bacon¹¹, S. Bocquet¹², D. Brooks⁵, D. Brout¹³, E. Buckley-Geer^{14,8}, D. L. Burke^{15,16}, A. Carnero Rosell^{17,7}, D. Carollo¹⁸, J. Carretero¹⁹, L. N. da Costa⁷, M. E. S. Pereira²⁰, J. De Vicente²¹, S. Deniz²², H. T. Diehl⁸, S. Everett²³, I. Ferrero²⁴, B. Flaugher⁸, J. Frieman^{8,25}, J. Gaior-Ende⁶, E. Gaztanaga^{27,11,28}, G. Giannini^{19,25}, K. Glazebrook²⁹, R. A. Hild³⁰, S. R. Hinton¹, D. L. Hollowood³², K. Honscheid^{33,34}, D. Jeltem³, R. Kessler^{14,25}, K. Kuehn^{35,36}, O. Lahav⁵, J. Lee³⁷, S. Lee²³, M. Lima^{38,7}, J. L. Marshall³⁹, I. M. Hernandez⁴⁰, R. Miquel^{41,19}, J. Myles⁴², A. Möller²⁹, R. C. Nichol¹¹, R. C. Ogando⁴³, A. Palmese⁴⁴, A. Pieres^{7,43}, A. A. Plazas Malagón^{15,16}, A. K. Romer⁴⁵, M. Sako³⁷, E. Sanchez²¹, D. Sanchez Cid²¹, M. Schubnell⁹, M. Smith⁴⁶, E. Suchyta⁴⁷, M. Sullivan⁴⁶, B. O. Sánchez^{48,49}, G. Tarle⁹, B. E. Tucker⁴, A. R. Walker⁶, N. Weaverdyck^{50,51}, and P. Wiseman⁴⁶,

(DES Collaboration)

Affiliations are listed at the end of the paper.



So many people from so many places that we had to put the places at the end of the paper!

Accepted XXX. Received YYY; in original form ZZZ

Here's the tl;dr...

We present a precise measurement of cosmological time dilation using the light curves of 1504 type Ia supernovae from the Dark Energy Survey spanning a redshift range $0.1 < z < 1.2$. We find that the width of supernova light curves is proportional to $(1+z)^b$, where the parameter b is the same as that of the first (Friedmann) approximation to the metric. We fit the emitted with a consistent duration Δt_{em} , and parameterising the observed duration as $\Delta t_{\text{obs}} = \Delta t_{\text{em}}(1+z)^b$, we fit for the form of time dilation using two methods. Firstly, we find that a power of $b < 1$ minimises the box scatter in stacked subsamples of light curves with different redshifts. In this analysis, we find $b = 1.003 \pm 0.005$ (stat) ± 0.010 (sys). Thanks to the large number of supernovae and large redshift range of the sample, this analysis gives the most precise measurement of cosmological time dilation to date. Our results are consistent with the predictions of general relativity, and provide the most stringent test of the expanding Universe hypothesis to date. We also find that the quality of the data from our collaboration, the Dark Energy Survey, this is the most precise detection of cosmological time dilation so far.

Here's the background:

Time dilation is a fundamental implication of Einstein's theory of relativity in an expanding Universe — the observed duration of an event, Δt_{obs} , should be longer than the intrinsic emitted (or rest-frame) duration, Δt_{em} , by a factor of one plus the observed redshift, z .

Cosmological time dilation is yet *another* prediction that can be traced back to Einstein! (1)

The idea of using time dilation to test the hypothesis that the Universe is expanding dates back as far as Wilson (1939) and was revisited

by Rust (1974). One of the first observational hints of time dilation was seen in the light curves of gamma-ray bursts (GRBs) (Paczynski et al. 1999). The duration of gamma-ray bursts (GRBs) was inversely proportional to their brightness. They used this to argue that at least some GRBs must be cosmological. The first measurement of cosmological time dilation using supernovae were made by Leibundgut et al. (1996) for a single supernova at $z \approx 0.3$ and Riess et al. (1997) for seven supernovae at $0.3 < z < 0.5$. Most relevant to this work, Riess et al. (2019) used the latest state-of-the-art in identifying and calibrating dilation in SNIa photometry. They used 35 supernovae in the redshift range $0.30 \leq z \leq 0.70$, to test a model of the Universe with no dilation and found $b \sim 1.07 \pm 0.06$.

* E-mail:ryan.white@uq.edu.au

width and time dilation, Foley et al. (2005) and Blondin et al. (2008) observed time dilation in the evolution of spectra of high-z Type Ia supernovae (SNe Ia). The former found inconsistency with the latter’s static universe model, finding $b = 0.97 \pm 0.10$. Most recently, Lewis & Brewer (2023) inferred $b = 0.97 \pm 0.09$ using the variability of 190 quasars out to $z \sim 4$. Despite these successes, there remains continued discussion of hybrid or static-universe models such as Tired Light (Zwicky 1929; Gupta 2023) that do not predict expansion-induced time dilation.

In this study, we measure cosmological time dilation using SNe Ia from the full 5-year sample released by the Dark Energy Survey (DES) (DES Collaboration et al. 2024), which contains ~ 1500 SNe Ia spanning the redshift range $z = 0.05$ – 1.5 . This is significantly larger and higher redshift than any sample of supernovae previously used for a time-dilation measurement. Such a large sample of SNe Ia is important to ensure that our results are robust enough. The redshift range is the ideal regime to robustly identify time dilation. Over half the DES sample (54%) have redshifts between $z = 0.5$ and 1.0 , while the previous gold-standard Pantheon+sample (Bautista 2019) and 37% in the Goldhaber analysis (Goldhaber 2001). Therefore the DES sample is likely to have a lower time dilation signal than 1.5 times longer than their rest frame durations (up to 2.2 times longer for those at $z \sim 1.2$). This means their time dilation signal should be significantly larger than the intrinsic width variation expected due to SNe Ia diversity in their subtypes.

We test the model that time dilation occurs according to,

$$\Delta t_{\text{obs}} = \Delta t_{\text{em}}(1+z)^b. \quad (2)$$

If Type Ia supernovae are the result of white dwarf stars exploding, these white dwarf stars are the super-compact remnant cores of stars that have shed their outer layers – kind of like the skeleton left over after we die. Some of these stars steal extra material from nearby stars while in their white dwarf phase. When they steal so much matter that they reach a critical mass (the Chandrasekhar mass) they explode! Since they all explode at this same mass, Type Ia supernovae all look pretty much the same no matter where they are!

(i) Firstly, we simply take all the light curves, divide their time axes by $(1+z)^b$ (so that the spectrum is redshifted) and the value of b that minimises the flux scatter.

(ii) Secondly, we take the shifted light curves and stack them to define a data-driven SN Ia ‘reference light curve’. Then for each individual SNe Ia we measure the observed light curve width (or ‘width’ in the sense of the FWHM) at various wavelengths. This allows us to see if the time-dilation occurs smoothly with redshift and the value of b that would be required. The result would be $w = (1+z)$ corresponding to $b=1$.

The first method is entirely data-driven and has no time-dilation assumption. In the second method, as a consistency check we create the stacked reference by dividing the time axis of the light curves by $(1+z)$. This method therefore includes an assumption of time-dilation in the form $w = (1+z)^b$. The consistency check on this assumption is justified by the result of the first method, the second method should strongly favour the first method. We note it is possible to remove any circularity by keeping the reference light curves in their rest frame and fitting to $w = ((1+z_{\text{target}})/(1+z_{\text{reference}}))^b$, with z_{target} and $z_{\text{reference}}$ being the redshifts of two different target supernovae; mathematically this is very similar to our approach but requires even more data. To further check that this method rules out no time dilation we re-test method two without de-redshifting the reference light curves; it dramatically fails the consistency check, see Appendix C.

This paper is arranged as follows. In Section 2 we discuss the use

of type Ia supernovae as standard candles, and the challenges that need to be taken into account when comparing SNe Ia light curves observed in different bands across different redshifts. In Section 3, we present the data used in this study, while Section 4 describe our approach of defining a reference light curve and the determination of the redshift dependence of the time dilation signal. We discuss our results in Section 5 and conclude in Section 6 that the null hypothesis of no time dilation is inconsistent with the data.



It's important to use the most distant supernovae possible for these types of studies. The further away a supernova is, the stronger the time dilation signal! This lets us find the signal amongst the noise.

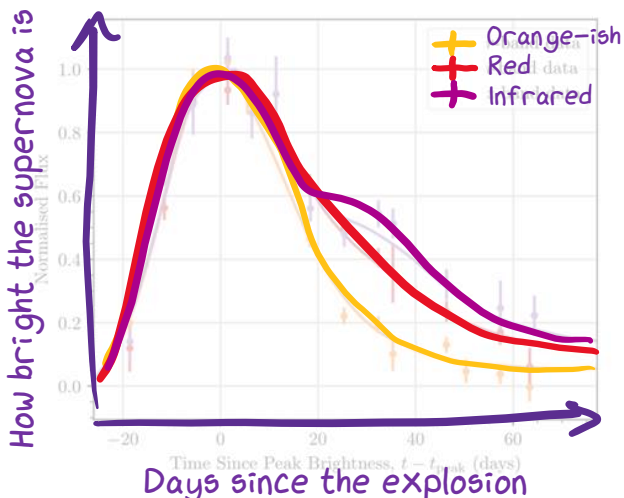
We want to be really sure about how much time dilation there is as we correct for this in cosmological analyses.

The presence of a time dilation signal in SNe Ia data tests the general relativistic prediction of an expanding universe having a factor of $(1+z)^b$ time dilation (Riess et al. 2008). This signal needs to be corrected for in supernova cosmology analyses (Taubenberger et al. 2016) and accurately quantifying the effect of time dilation is foundational to our cosmological model, especially considering the continued discussion of hybrid or static-universe models such as Tired Light (Zwicky 1929; Gupta 2023) that do not predict expansion-induced time dilation.

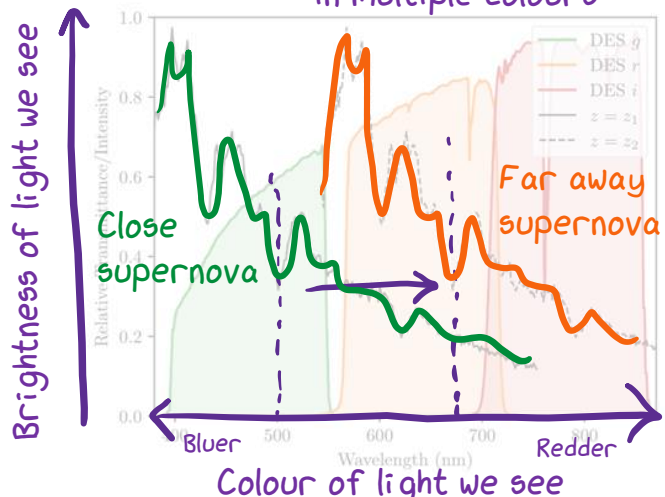
2.1 The importance of colour

Type Ia are known to spectrally evolve over the duration of their ~ 70 -day bright period. The early spectrum is relatively blue with spectral features dominated by transitions from intermediate mass elements. The spectrum then reddens on the order of days from heading towards emission lines and the peak of the spectrum (Filippenko 1997). Previous papers have described the redward evolution of SNe Ia spectra over time (Takanishi et al. 2008; Marin et al. 2012; Branch & Wheeler 2014) while photometric evidence of this phenomenon is seen in the light curve peaking later in redder bandpasses than in bluer ones (in Figure 1) for a source in the rest frame optical. As such, the photometric behaviour of a light curve is dependent on the rest-frame wavelength range observed. It is therefore important that a good approximation to a typical high-z SN Ia observed in a redder band should have the same photometric and spectral characteristics as a medium-z SN Ia observed in a bluer band (Figure 2). Since our photometric bands are fixed, they sample different rest-frame wavelength ranges as the supernovae are redshifted. Therefore, it is critical to design a method that ensures time dilation measurements compare light curves measured at similar rest-frame wavelengths.

¹ A note on language: The phrase ‘rest-frame’ wavelengths arises from the usual assumption that redshifts are due to recession velocities. The fact red-



↑ This is what our data looks like! We have 'light curves' of 1504 unique supernovae, in multiple colours



The expanding Universe makes distant blue light appear red to us we call this 'redshift'. This plot shows that the colour spectrum of a supernova that's far away is redshifted compared to one that's close by

shifts occur is not in question here (so it is fine to use $(1+z)$ to calculate matching rest-frame wavelengths, and this contains no time-dilation assumption). The question is whether that redshift arises due to a recession velocity, which would also cause time-dilation.

Type Ia supernovae aren't actually as consistent as I've been letting on, but light curves are all similar. One dissimilarity between SNe Ia is the width of the light curve. The width of the light curve is up to ~ 20% that is separate from time dilation and strongly correlated with the redshift. This probably means that the physical data at such high redshifts we can simply treat this inhomogeneity as noise. The stretch variation between SNe Ia essentially acts as a bias in our analysis. This does not affect the overall trend of light curve width against redshift, but it does affect the slope. The main effect is that the relation is less weak to begin with if model dependence is removed. As long as there is a representative sample of the entire population, the effect of this bias is small enough that it does not affect time-dilation without bias. However, Malmquist bias can influence the result since brighter supernovae have wider light curves. If faint supernovae are under-represented at high-redshifts one might expect a slight bias toward a higher inferred time dilation at high-redshift. This actually has the same effect as time dilation and this makes our analysis a bit trickier. Luckily the Dark Energy Survey found so many supernovae of all types that we don't need to correct for this; it all averages out. Even if it didn't average out, this would affect is not as strong as the time dilation. Previous studies (e.g. Nicolis et al. 2021) have also found that the DES SN5YR sample out to $z = 1.1$ (see also Fig. A2), meaning that the stretch-luminosity relation should have a negligible effect on our results.

What data do we have?

The 4m Blanco Telescope at the Cerro Tololo Inter-American Observatory observed thousands of supernovae for the Dark Energy Survey. 1504 of them made the cut for this paper!

² FLUXCALERR is the Poisson error on ELHXCAL, which is the variable used for flux in SNANA corresponding to $\text{mag} = 27.5 - 2.5 \log_{10}(\text{ELHXCAL})$.

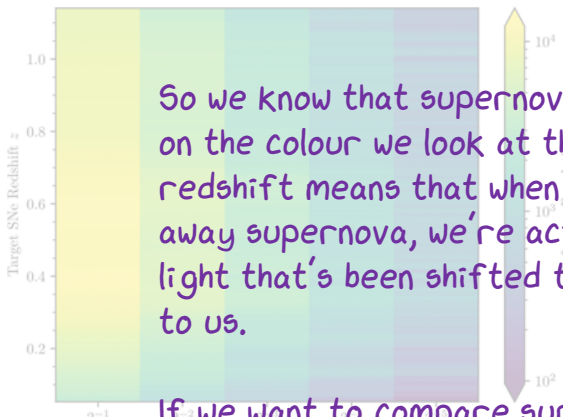


Figure 3. For each of the SNe Ia in our sample, we constructed a reference light curve with a $\delta \leq 2$ parameter according to Equation 3, with λ_f band FWHM. We counted how many data points populated the reference curves (i.e. the number of *points* in Fig. 3; for example) changing δ in integer steps of powers of 2. This shows that for a target light curve in some SN measured in the observer frame ℓ band, and is largely similar for the different bands differing by a factor of 2 along the vertical axis. That is, an analogous plot in a bluer band would see the colour distribution shifted downwards in target redshift and a redder band upwards.

high redshift (whose observations had comparatively low FLUXCAL). In the analysis, we did not attempt to fit SNe light curve widths if their light curve had fewer than 5 data points and if their reference curve had fewer than 100 data points (discussed in Section 4). This was done on a per-band basis; we estimated the width of each SN light curve in each band where it satisfied these criteria. Individual light curves were also omitted from the analysis if the χ^2 width fitting did not converge. All together, after these quality cuts we were left with width measurements of 1504 unique SN Ia across the dataset.

What do *we* do in the paper?

4 FITTING SUPERNOVA PHOTOMETRY TO A REFERENCE LIGHT CURVE

If time dilation is real, we should see that supernovae take longer at higher redshift (from our perspective). That means that if we literally stack light curves from the 1504 individual light curves to fit their own *unique* reference curve composed of all the imaging photometry in the DES dataset. The length of the reference curve is the inverse of said scaling factor, and this can be found for each of the 1504 individual light curves. This is a template-like fitting method in that we do not assume the shape of a light curve but instead let the data from other SNe compose the template-like reference curve.

Our method is unique in that we use *only* the data from the Dark Energy Survey—no other supernovae were hurt in the making of this paper.

4.1 Reference curve construction

The main functionality of this method is to use the photometric data of many SNe to automatically create a reference light curve unique

to any one target SN. The target SN is the SN whose width we are trying to measure.

Since the shape of a SN Ia light curve is dependent on the rest-frame effective wavelength which it is observed (Fig. 1; see also Takanashi et al. 2008; Blondin et al. 2012), the reference photometry must be composed of many light curves that have the same (or very similar) intrinsic shape as the target SN. Hence, we must choose reference photometry that samples the same rest-frame effective wavelength as the target light curve. This plot is Figure 2, where, for example, we might compare a low- z supernova in some band to a high- z supernova in another band, both with the same (or similar) rest frame effective wavelength. We can compare the photometry between the two events provided that their rest-frame effective wavelength (and hence their light curve shape/evolution) is alike.

We want to compare supernova light curves across different redshifts, we need to account for these effects. We proposed using a mathematical selection function* to carefully choose light curves at certain redshifts and in certain colours so that we get a sample that should all have the same shape. An arrow from the text 'We proposed using a mathematical selection function*' points to this equation.

To find relevant light curves to populate the reference curve, we pick all light curves out of a calculated redshift range to fit a single (target) SN light curve at redshift z imaged in a band of central wavelength λ_f , we can populate the reference curve with SNe within the redshift range

$$\frac{\lambda_r(1+z)}{\lambda_f} - \delta \frac{\Delta\lambda_f}{\lambda_f} \leq 1 + z_r \leq \frac{\lambda_r(1+z)}{\lambda_f} + \delta \frac{\Delta\lambda_f}{\lambda_f} \quad (3)$$

This equation essentially says that if we want to compare with a supernova at a very high redshift, we need to collect light in a redder filter so that we're seeing the same type of stuff!

We show in Fig. 3 the number of points in the reference curves (the reference curve population) for all the DES SNe with a variable δ parameter. Ideally, this δ parameter should be as small as practical to ensure that the reference curve is consistent in shape (i.e. the spread of rest frame effective wavelengths is small). In practice, we find a value of $\delta = 2$ is the minimal value that provides a large enough reference population for high/low redshift SNe (on the order of $\sim 10^3$ needed to satisfy the Section 3 criteria at $z > 0.5$). As we increase δ (and therefore the number of SNe in the DES-SN sample), we note that the reference population is large (we have up to $\sim 10^4$ points).

After populating the reference curve with data points, we then normalise the photometry in flux, as the curve is populated with curves that have different peak fluxes. The reference light curve must be homogeneous in flux. To do this, we utilised the peak flux in the SALT3 model light curves provided for each SNe. The data in each constituent curve is normalised by this value before being added to the reference. For convenience we also use the time of peak brightness given by SALT3 as the reference point about which to stretch the light

*For literal astrophysics, we're kind of light on the math in this paper!

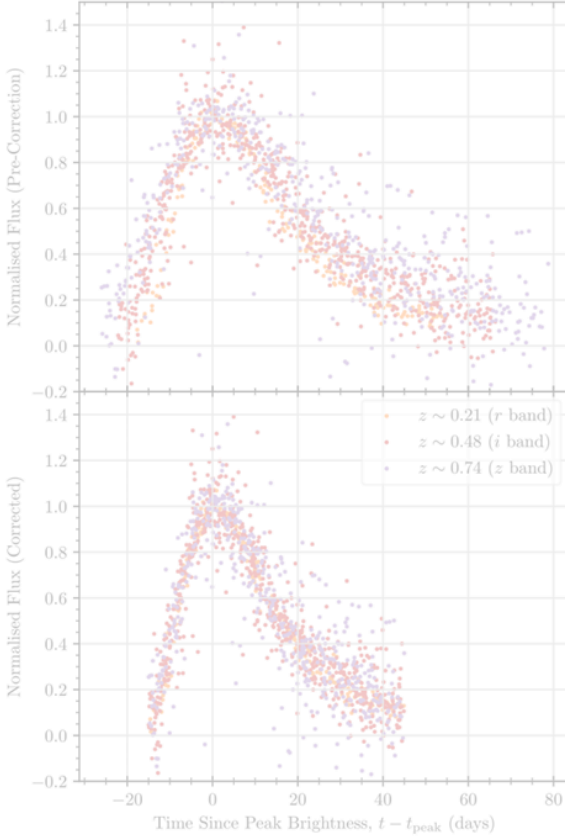


Figure 4. For a target SN Ia at $z \approx 0.48$, the i -band reference curve consists of data from the r , i , and z bands. These data are chosen at redshifts according to equation (3) (and visually shown in the left plots of Fig. 6). *Top:* the data in different bands are not in phase (in the observer frame). It is visually obvious that light curves appear wider in time at higher redshift. *Bottom:* after a $(1+z)$ correction to the SN Ia light curves, we see a consistent trend across all bandpasses and time. This alone is evidence for some degree of time-dilation.

curves (see equation 5). These are the only uses of SALT3 information and we expect that the same time dilation signal would be obtained in the data with any other consistent normalisation measures.

4.2 First measure of time dilation: minimising scatter in the reference curve

After the flux of the reference curve is normalised, we see that the different bandpass data in the curve are temporally stretched (see the colour gradient of the top plot in Fig. 4). As the redder bandpasses are sampled at higher redshift, this is an immediate indication of time dilation. Without assuming our expected cosmological time dilation of $(1+z)$, we can scale the data in *all* of the reference curves by a factor of $(1+z_j)^b$, where z_j is the redshift of each constituent curve in a reference and b is a free parameter. We posit that minimising the flux dispersion in the reference curve is analogous to finding the optimal temporal scaling, simultaneously minimising the dispersion in time. Hence, finding the value of b that minimises the flux scatter gives us our correction factor.

To investigate this, we generated reference curves for each of the

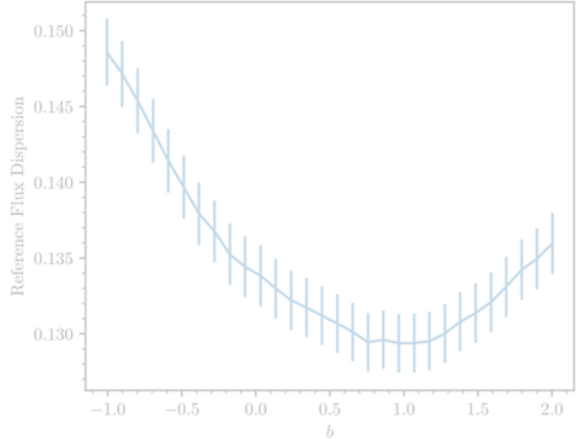


Figure 5. By scaling the reference photometry in time according to $(1+z)^b$ for some free parameter b , we find $b \sim 1$ minimises the reference flux dispersion across the entire SNe sample. The reference flux dispersion represents the median dispersion of flux across the entire sample of normalised reference light curves in each band (here averaged for the riz bands), where the errorbars indicate one standard deviation in these values. We note that this figure yields a signal of $(1+z)$ time dilation in the DES dataset, independent of the rest of the analysis.

target SNe per observing band and scaled the data in time according to the aforementioned relation in terms of b (Fig. 4 shows this scaling for $b = 1$ as an example). Then, we binned the timeseries data into 30 equal-width time bins and found the standard deviation of the flux within each bin. We calculated the median of these 30 standard deviations as a representative estimate of the total flux scatter for that reference curve with that tested b value. We then took the median of those results across all the SN reference curves as our estimate of the dispersion for that b , which is shown in Fig. 5. That is, our reference flux dispersion is

$$\sigma_{\text{rf}}(b) = \text{Med} \left(\{ \{ \text{Med}(\sigma_{ij}(b)) | \forall j \in (1, \dots, 30) \} | \forall i \in (1, \dots, N_{\text{sn}}) \} \right) \quad (4)$$

for N_{sn} supernova light curves in that band, and $\sigma_{ij}(b)$ being the flux standard deviation of the i th light curve in the j th timeseries bin. This process was repeated for each of the riz observing bands, omitting the g band due to the smaller number of SNe. We crudely estimate the error (for each b) in this method as being the standard deviation of the median dispersions across all light curves. We find an optimal scaling corresponding to $b \sim 1$ (Fig. 5) across the entire dataset, which is the expected dilation factor of $\sim (1+z)$.

If there was no time dilation we would expect the minimum dispersion in the reference curve to be at $b \sim 0$ (i.e. no time scaling) in Fig. 5. The fact that we find $b \approx 1$ is evidence for time dilation of the expected form. This a rough but completely model independent measure of time dilation and it is the paper's first main result.

4.3 Second measure of time dilation: Finding each light curve width

After constructing the reference curves for a target SN, we are ready to fit for the width, w , of each individual target light curve and look for a trend with redshift. This method enables a more precise measure of b .

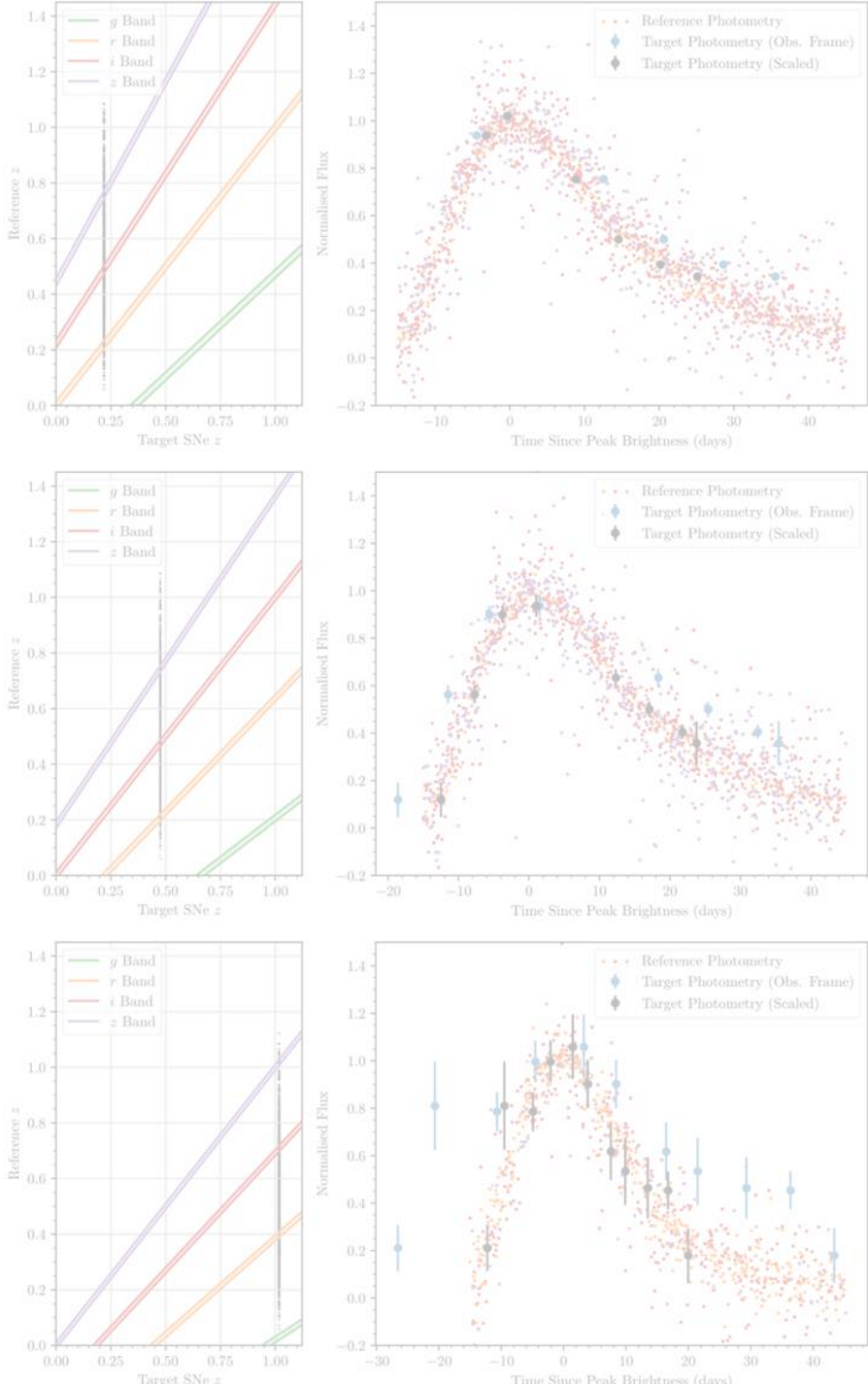


Figure 6. We show the reference curve construction and subsequent target SN fit for 3 SNe at redshifts $z = 0.22$, $z \approx 0.43$, and $z \approx 1.02$ and in fitting bands r , i , and z respectively (in descending order). The left plots show the allowed ranges for reference curve SN sampling given the target redshift (and $\delta = 2^{-4}$). The vertical line of dots is plotted at the target SN redshift, with each dot representing the redshift of a DES supernova (vertical axis). The dots that fall in the narrow coloured bands are the SNe that make up the reference population, as those data all share approximately the same rest-frame wavelength in their respective bands. The right plots show the constructed $(1+z)$ time-scaled reference curve (small coloured points) with respect to the target SN photometry (blue points) and subsequent target photometry scaled on the time axis to fit the reference (best-fit widths of 1.42, 1.49, and 2.17 respectively). Due to the statistics associated with such large reference curve populations, the contribution of any individual reference point uncertainty to the overall reference curve uncertainty is negligible and not plotted; the uncertainty in the target data has a much higher contribution to the uncertainty in the fitting.

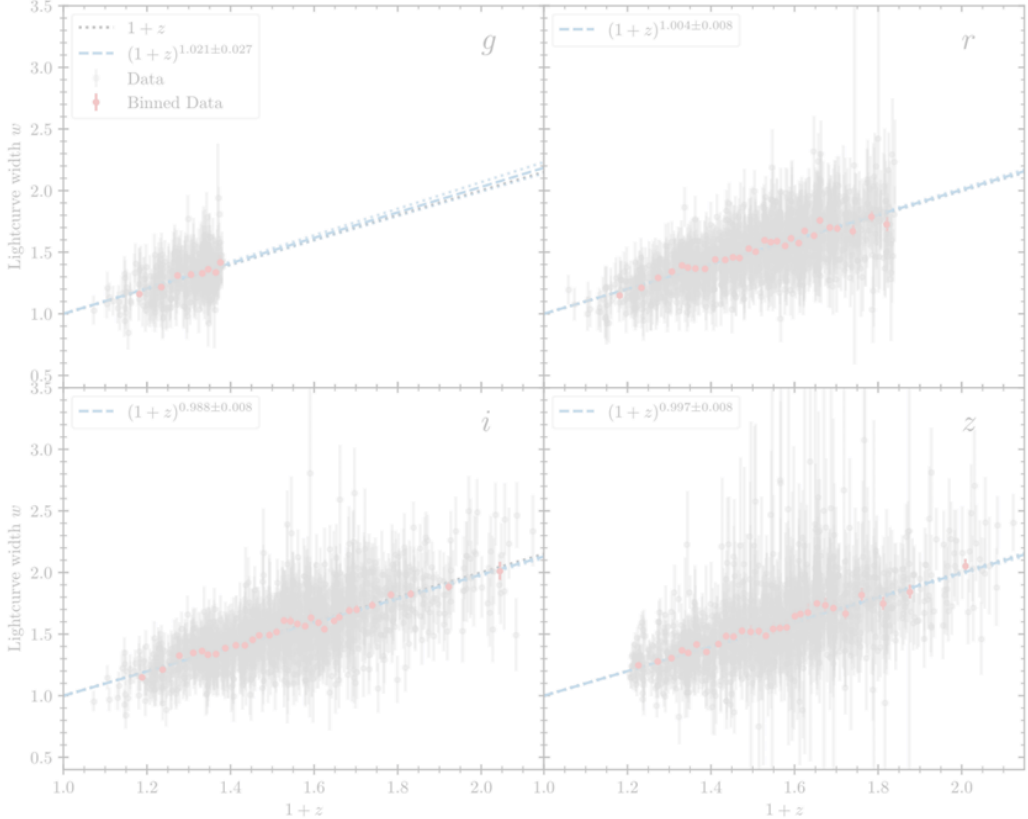


Figure 7. Using the reference-scaling method described in Section 4.3, we plot the fitted SNe widths of light curves observed in the g , r , i , and z bands (left to right, top down respectively). The lines of best fit (blue dashed) are in excellent agreement with the expected $(1+z)$ time dilation (black dotted). The binned data are purely to visualise rough trends in 50 data point bins. 361 SNe in the g band passed the quality cuts described in Section 3, while the r band has 1380 SNe, the i band 1465, and the z band 1381. The reduced chi-square values, χ^2_{ν} , of each fit (left to right, top down) are 0.537, 0.729, 0.788 and 0.896 respectively.

We first normalise the target data to the peak flux using the SALT3 fit (as with the reference curves). The free parameter in the fit is the scaling parameter $1/w$, whereby changing this value would stretch and squash the data relative to t_{peak} (the time since peak flux) until the χ^2 is minimised. That is, we assume the SN Ia light curve of the i th supernova is of a mathematical form similar to that described in Goldhaber et al. (2001),

$$F_i(t) \simeq f_i \left(\frac{t - t_{\text{peak}}}{w} \right) \quad (5)$$

and change w until the data most closely matches the reference. Here, $f_i(t)$ corresponds to the i th target light curve; $F_i(t)$ corresponds to the i th reference curve where each point is now scaled in time by $(1+z)$ relative to t_{peak} as per the results of Section 4.2.

To fit the target light curve width using its reference curve, we minimised the χ^2 value of the differences in the target flux compared to the median reference flux in a narrow bin around time values of the target photometry. That is, for each target light curve we minimised

$$\chi^2_i = \sum_j^{N_p} \frac{(f_{ij} - \text{Med}\{F_i(t) \mid \forall t \in [t_{ij}/w - \tau, t_{ij}/w + \tau]\})^2}{\sigma_{ij}^2} \quad (6)$$

for N_p number of points in the i th target SN light curve (f_i). The points in the reference curve (F_i) bin that are averaged and compared

to each target SN flux value (f_{ij} – with error σ_{ij}) are selected within the time range $[t_{ij}/w - \tau, t_{ij}/w + \tau]$; here t_{ij} is the time since peak brightness of each target data point scaled by the fitted width w , and τ is the half bin width either side of the central time value t_{ij} .

During the fitting process, the bounds of this narrow bin around each time value changes as the target data is scaled in time but remains the same width. We chose a bin width, 2τ , of 4 rest-frame days (i.e. $\pm\tau = \pm 2$ of a central value); ideally this would be as low as practical to maximise intrinsic similarity between the target data point position and the reference curve slice, but needs to be large enough to provide a sufficiently populated sample of the reference to compare to. We find that a width of 4 days (just under the width of a minor tick span in Fig. 4) is low enough that the reference curve does not significantly change in flux but still contains enough points even for high/low redshift target SNe with small reference populations. With this $\tau = 2$ value we find $\gtrsim 50$ data points per time slice at the highest and lowest redshifts, where a $\tau = 1$ yields a prohibitively small $\lesssim 20$ data points per slice even in the most well sampled photometric band (i -band).

In fitting the data, we did not include any target SN data points that extended past the maximum time value in the reference curve; the late-time light curves of SNe dwindle slowly and are less constraining for width-measurements than those near the peak. We also omitted any points that had observation times prior to the first reference curve point from the fitting procedure.

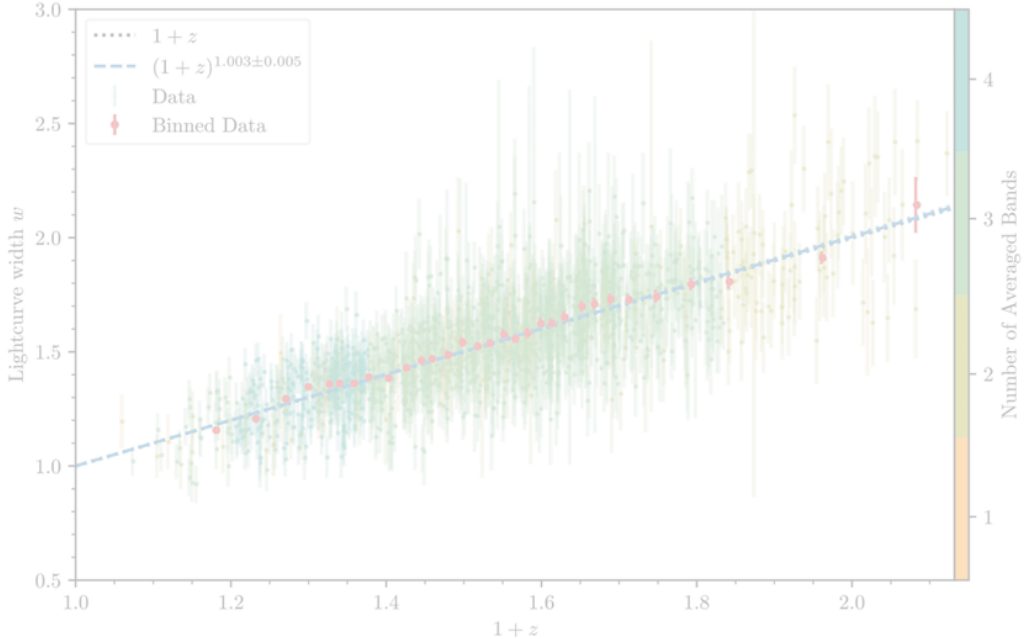


Figure 8. We show here the width value for each SNe averaged across all available bands. Since cosmological time dilation is independent of the observed band of any SN, we are able to average the widths over observed bands to form a more robust estimate of the light curve width. This relationship of $(1+z)^{1.003\pm 0.005}$ time dilation (reduced chi-square $\chi^2_{\nu} \approx 1.441$) is comprised of the 1504 unique SNe across the 4 bandpasses, where the error bars here are the Gaussian propagation of the errors in each band. Points are coloured according to how many bandpasses were used in computing the averaged width. A linear model fit to the data recovers $w = (0.988 \pm 0.016)(1+z) + (0.020 \pm 0.024)$ (with the same χ^2_{ν} to 4 significant figures), consistent with our power model fit above.

We note that this method of fitting is not fundamentally limited to target SN data with pre-peak brightness observations in each band. Given enough target data (on the order of several well spaced points in time), the mapping of this data to the corresponding reference curve phases is unique regardless of whether pre-peak data is available.

The uncertainty in each estimated width was found via Monte Carlo uncertainty propagation, where the target data was resampled 200 times according to its Gaussian error; for each iteration we fit the width and the final error is the standard deviation in these widths. To provide some measure of the error in the reference curve, we imposed an error floor of $\sigma_m(1+z)$ on the Monte Carlo uncertainty, for σ_m representing the median (normalised) flux dispersion in the reference curve. The σ_m dependence is from our rationale that the fit width is only as good as the quality of the reference curve, and the $(1+z)$ dependence arises from our scaling of the reference curve.

An example of how a reference curve is created is shown in Fig. 4. We note the difference in the reference curve timescale before and after $(1+z)$ correction, and the larger dispersion in flux between the points at any one time prior to correction. Several examples of width fitting and reference curve construction for low, medium, and high redshift target SNe (in the context of the DES-SN sample) are shown in Fig. 6.

We note that while the width fitting for the whole dataset was calculated in all four DECam bands, only the i band data encompasses the entire redshift range of the DES-SN sample. Due to the spectral shifting inherent in redshifted data, the g and r filters are unable to detect SNe at sufficiently high redshift ($z \gtrsim 0.4$ and $z \gtrsim 0.85$ respectively) as the observed wavelengths shift to lower emitted wavelengths (see Fig. 2 of DES Collaboration et al. 2024) and become fainter as a re-

sult. Fig. 6 shows that fitting $z \lesssim 0.2$ SNe in the z -band would require negative redshifted SNe in the other bands to populate the reference; hence there is an inherent redshift floor for z -band fits leaving the i -band as the only suitable bandpass for the entire redshift range.

The widths obtained in all four bands separately are shown in Fig. 7. We see the truncated g , r and z band data, and fit widths consistent with the expected $(1+z)$ relationship across all bands. The averaged widths of all the bands are shown in Fig. 8, again showing excellent agreement with the $(1+z)$ expected theory.

As mentioned in the introduction, this method has an element of circularity because we de-time-dilated the observed light curves to generate each reference light curve. As a cross-check to ensure that we are not just getting the answer we put in we repeated the analysis *without* de-redshifting the data. This effectively makes the reference light curves more noisy and wider (like the top plot of Fig. 4). If time dilation is absent we should get a consistent $b = 0$ fit in this case. However, if $(1+z)$ time dilation is present we should find a slope inconsistent with $b = 0$ and an intercept offset from $w = 1.0$ (because the reference light curve will itself be time-dilated). We find, as expected, that the $b = 0$ result is excluded strongly by this test (see Appendix C and Fig. C1).

5 DISCUSSION

As we see in Fig. 7, there is a clear and significant non-zero time dilation signature in the DES SN Ia dataset, conclusively ruling out any static universe models. Our method described in Section 4 detects a time dilation signature in all of the g , r , i , and z DECam bandpasses

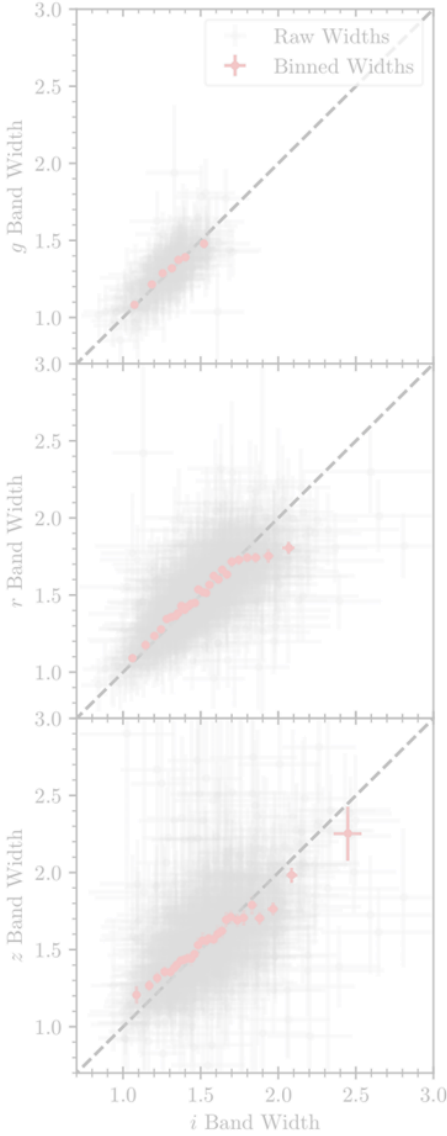


Figure 9. Since most SNe were observed in multiple bands, the fit widths in each band for each SNe should be intrinsically correlated as they arise from the same event. Hence, the widths for the same target SN should show some agreement between bands. We plot their agreement relative to the i band which had the most SNe pass the quality cuts. Each of the data points here corresponds to a width in Fig. 7 of bands g , r , or z against the i band widths. A 1:1 dashed line is shown to represent perfect agreement and binned points are plotted to represent the trends in the agreement.

as expected. The power-law fits to the data in each bandpass are all consistent with the expected $(1+z)$ law to within 2σ .

Since there is a well documented stretch-luminosity relationship in Ia light curves (Phillips 1993; Phillips et al. 1999; Kasen & Woosley 2007), it is possible that Malmquist bias could skew the data to larger widths at high redshift where we may not see the less-luminous SNe. Regardless, this does not greatly influence the quality of our fits since the DES SN data extend to such high redshifts that the

intrinsic dispersion in widths is significantly smaller than the time dilation signal. In fact, we find that the standard deviation in the width residuals (i.e. of $w_i - (1+z_i)^{1.003}$ for all SNe) within Fig. 8 is only ~ 0.15 (which includes observational uncertainty as well as intrinsic stretch dispersion). At $z \sim 1$ we would expect a time dilation factor of ~ 2 and so the contribution of time dilation far outweighs the intrinsic light curve stretch in the supernova population.

Nicolas et al. (2021) (see also Howell et al. 2007) showed that there is a 5σ ‘redshift drift’ in the stretch of their unbiased multi-survey sample of SNe Ia; that is, higher redshift SNe Ia tend to be intrinsically wider. Although we do not see this trend in the DES-SN5YR sample, we nevertheless quantify how such a drift could affect a time dilation measurement (Appendix A). Given that the drift is so small, we find its impact would be minimal even if it is hidden in the data ($|\Delta b| \lesssim 0.02$).

As a test of the robustness of our method, we reran all the width-fitting code with a requirement of pre-peak observations in each light curve. At *most*, this changed the power law fit by $\Delta b = -0.004$ for the g band. The calculated b values in the other bands were increased by one or two thousandths (including the averaged fit of Fig. 8), or not at all. Interestingly, including this pre-peak restriction reduced our number of unique SNe widths by only 24 in total. This reduction does not let us conclusively say if this method is robust at fitting light curves without pre-peak data, and future analyses may look at purposefully degrading the dataset (e.g. by manually removing pre-peak data) to investigate this.

Our method creates a unique reference light curve for each SN as a function of bandpass and redshift, and so we are able to infer a time dilation signature no matter the photometric band. This is in contrast to Goldhaber et al. (2001) who showed time dilation in the B -band and suggested it would hold in the other bands (see also Wang et al. 2003). Fig. 9 compares the calculated widths in each band relative to the i -band sample (which has the most SNe of any DECam band). The apparent discrepancies toward high widths in the i band might be explained by dust effects or noise domination in the observation of high redshift supernovae (Möller et al. 2022, 2024). With that said, we see generally broad agreement between the widths in the different bands as expected of our source wavelength-flexible model.

To avoid de-redshifting reference light curves we devised another method, similar in concept to method two above, that would yield a posterior distribution of b . This entailed generating a reference curve *without* first scaling it in time (as in the second method), and fitting target data with a free b (as opposed to w) to the reference data of each constituent band. That is,

$$\Delta t_{\text{target}} = \Delta t_{\text{reference}} \left(\frac{1 + z_{\text{target}}}{1 + z_{\text{reference}}} \right)^b \quad (7)$$

and we attempted this with the same χ^2 minimisation procedure as in equation (6). With this method we tried 1) separating the reference data into the constituent bands, fitting the χ^2 to each band reference and minimising the weighted sum of these χ^2 . The sum was weighted according to how many points made up each constituent band reference curve, and this method is preferred as it assesses the fit to all bands fairly. We also tried 2) fitting b using the χ^2 on the entire scaled reference (i.e. all bands together), but this is not preferred as the reference is not necessarily composed of points equally sampled from all bands and so can prefer fitting b towards a single bands reference (i.e. a particular redshift). This method was abandoned overall as we did not have enough data (even with the DES dataset) to accurately fit χ^2 values to each band. We expect that this procedure would be viable in the future with an even larger SNe Ia dataset of a comparable redshift distribution, or by using a Bayesian approach

(which will be the topic of future work). We instead performed the analysis with flux-scatter-minimisation and width-fitting methods as the former does not rely on fitting target SN data and the latter fits to a unified (in phase) reference curve composed of all available bands.

Finally, in the spirit of the results of Goldhaber et al. (2001), we similarly state that our method with the DES dataset would disfavour the null hypothesis of no cosmological time dilation to a $1.003/0.005 \approx 200\sigma$ significance. (If σ values were still meaningful at that extreme!) Our uncertainty estimate is a statistical uncertainty only; in Appendix A we look at a possible systematic effect due to evolution of the stretch of supernova light curves as a function of redshift. We find it to be small, with a likely upper bound of $\sigma_b^{\text{sys}} \approx 0.01$. Even with an upper limit to the uncertainty of $\sigma_b^{\text{sys}} + \sigma_b^{\text{stat}} \approx 0.015$ this remains the most precise constraint on cosmological time dilation.

6 CONCLUSIONS

Using two distinct methods, we have conclusively identified $(1+z)$ cosmological time dilation using the multi-band photometry of 1504 SNe Ia from the Dark Energy Survey that met our quality cuts. We make this detection with the most model-independent methods yet in the literature and with the largest survey of high redshift supernovae.

For both methods, we create a ‘reference curve’ unique to each supernova (and each bandpass) which describes the expected light curve shape without accounting for the stretch variation associated with SN Ia subtypes. Doing this relied on the scale of the available DES data (the number of SNe, the frequency of imaging, and the redshift range) and would not be possible with a significantly smaller survey. Creating this reference curve only relies on the assumption that SNe Ia should be standard candles/clocks.

Using this reference curve we show an inherent preference of $\sim (1+z)^1$ time dilation in the data, first by minimising the flux scatter in the data via a redshift-dependent temporal scaling, and then with a more traditional light curve width estimation. The latter allows for numerical estimates with uncertainty with which we obtain a factor of $(1+z)^{1.003 \pm 0.005}$ time dilation signature – the most precise constraint on cosmological time dilation yet.

We discuss factors and choices that affect our fits and notably see no indication that Malmquist bias or light-curve stretch significantly impacts our results. Our results infer a cosmological time dilation signature aligning strongly with the expected theory, corroborating past findings (Leibundgut et al. 1996; Goldhaber et al. 2001; Blondin et al. 2008; Lewis & Brewer 2023) with more SNe and at a higher redshift than ever before.

ACKNOWLEDGEMENTS

RMTW, TMD, RCa, SH, acknowledge the support of an Australian Research Council Australian Laureate Fellowship (FL180100168) funded by the Australian Government. AM is supported by the ARC Discovery Early Career Researcher Award (DECRA) project number DE230100055.

Funding for the DES Projects has been provided by the U.S. Department of Energy, the U.S. National Science Foundation, the Ministry of Science and Education of Spain, the Science and Technology Facilities Council of the United Kingdom, the Higher Education Funding Council for England, the National Center for Supercomputing Applications at the University of Illinois at Urbana-Champaign, the Kavli Institute of Cosmological Physics at the University of Chicago, the Center for Cosmology and Astro-Particle Physics at

the Ohio State University, the Mitchell Institute for Fundamental Physics and Astronomy at Texas A&M University, Financiadora de Estudos e Projetos, Fundação Carlos Chagas Filho de Amparo à Pesquisa do Estado do Rio de Janeiro, Conselho Nacional de Desenvolvimento Científico e Tecnológico and the Ministério da Ciência, Tecnologia e Inovação, the Deutsche Forschungsgemeinschaft and the Collaborating Institutions in the Dark Energy Survey.

The Collaborating Institutions are Argonne National Laboratory, the University of California at Santa Cruz, the University of Cambridge, Centro de Investigaciones Energéticas, Medioambientales y Tecnológicas-Madrid, the University of Chicago, University College London, the DES-Brazil Consortium, the University of Edinburgh, the Eidgenössische Technische Hochschule (ETH) Zürich, Fermi National Accelerator Laboratory, the University of Illinois at Urbana-Champaign, the Institut de Ciències de l’Espai (IEEC/CSIC), the Institut de Física d’Altes Energies, Lawrence Berkeley National Laboratory, the Ludwig-Maximilians Universität München and the associated Excellence Cluster Universe, the University of Michigan, NSF’s NOIRLab, the University of Nottingham, The Ohio State University, the University of Pennsylvania, the University of Portsmouth, SLAC National Accelerator Laboratory, Stanford University, the University of Sussex, Texas A&M University, and the OzDES Membership Consortium.

Based in part on observations at Cerro Tololo Inter-American Observatory at NSF’s NOIRLab (NOIRLab Prop. ID 2012B-0001; PI: J. Frieman), which is managed by the Association of Universities for Research in Astronomy (AURA) under a cooperative agreement with the National Science Foundation.

The DES data management system is supported by the National Science Foundation under Grant Numbers AST-1138766 and AST-1536171. The DES participants from Spanish institutions are partially supported by MICINN under grants ESP2017-89838, PGC2018-094773, PGC2018-102021, SEV-2016-0588, SEV-2016-0597, and MDM-2015-0509, some of which include ERDF funds from the European Union. IFAE is partially funded by the CERCA program of the Generalitat de Catalunya. Research leading to these results has received funding from the European Research Council under the European Union’s Seventh Framework Program (FP7/2007-2013) including ERC grant agreements 240672, 291329, and 306478. We acknowledge support from the Brazilian Instituto Nacional de Ciéncia e Tecnologia (INCT) do e-Universo (CNPq grant 465376/2014-2).

This manuscript has been authored by Fermi Research Alliance, LLC under Contract No. DE-AC02-07CH11359 with the U.S. Department of Energy, Office of Science, Office of High Energy Physics.

DATA AVAILABILITY

The data are available on Zenodo and GitHub as described in the DES supernova cosmology paper (DES Collaboration et al. 2024) and DES-SN5YR data release paper (Sanchez et al. 2024). The generated width fits and associated uncertainties for all 1504 SNe are included in the analysis GitHub (see Code Availability section), as are supplementary plots not included in the paper.

CODE AVAILABILITY

Our code in all analysis and plotting relied on the open source Python packages NumPy (Harris et al. 2020), Matplotlib (Hunter 2007), Pandas (pandas development team 2023), and SciPy (Virtanen et al.

2020) – specifically the Nelder-Mead algorithm described in [Nelder & Mead \(1965\)](#).

The code used to generate the width fits/reference curves and all associated figures is available at github.com/ryanwhite1/DES-Time-Dilation.

REFERENCES

- Abbott T. M. C., et al., 2018, *ApJS*, **239**, 18
 Blondin S., et al., 2008, *ApJ*, **682**, 724
 Blondin S., et al., 2012, *AJ*, **143**, 126
 Branch D., Wheeler J. C., 2017, Observational Properties. Springer Berlin Heidelberg, Berlin, Heidelberg, pp 483–517, doi:[10.1007/978-3-662-55054-0_20](https://doi.org/10.1007/978-3-662-55054-0_20), https://doi.org/10.1007/978-3-662-55054-0_20
 Brout D., 2019, in KITP Conference: Tensions between the Early and the Late Universe, p. 26
 Carr A., Davis T. M., Scolnic D., Said K., Brout D., Peterson E. R., Kessler R., 2022, *Publ. Astron. Soc. Australia*, **39**, e046
 DES Collaboration et al., 2024, arXiv e-prints, p. arXiv:2401.02929
 Filippenko A. V., 1997, *Annual Review of Astronomy and Astrophysics*, **35**, 309
 Flaugher B., et al., 2015, *AJ*, **150**, 150
 Foley R. J., Filippenko A. V., Leonard D. C., Riess A. G., Nugent P., Perlmutter S., 2005, *ApJ*, **626**, L11
 Goldhaber G., et al., 1997, Observation of Cosmological Time Dilatation Using Type Ia Supernovae as Clocks. Springer, Dordrecht, pp 777—784, doi:[10.1007/978-94-011-5710-0_48](https://doi.org/10.1007/978-94-011-5710-0_48)
 Goldhaber G., et al., 2001, *ApJ*, **558**, 359
 Gupta R. P., 2023, *Monthly Notices of the Royal Astronomical Society*, **524**, 3385
 Guy J., et al., 2007, *A&A*, **466**, 11
 Harris C. R., et al., 2020, *Nature*, **585**, 357
 Howell D. A., Sullivan M., Conley A., Carlberg R., 2007, *ApJ*, **667**, L37
 Hoyle F., Fowler W. A., 1960, *ApJ*, **132**, 565
 Hunter J. D., 2007, *Computing in Science & Engineering*, **9**, 90
 Kasen D., Woosley S. E., 2007, *ApJ*, **656**, 661
 Kenworthy W. D., et al., 2021, *ApJ*, **923**, 265
 Kessler R., et al., 2015, *AJ*, **150**, 172
 Leibundgut B., Sullivan M., 2018, *Space Sci. Rev.*, **214**, 57
 Leibundgut B., et al., 1996, *ApJ*, **466**, L21
 Lewis G. F., Brewer B. J., 2023, *Nature Astronomy*,
 Matheson T., et al., 2008, *AJ*, **135**, 1598
 Möller A., de Boissière T., 2020, *MNRAS*, **491**, 4277
 Möller A., et al., 2022, *MNRAS*, **514**, 5159
 Möller A., et al., 2024, arXiv e-prints, p. arXiv:2402.18690
 Müller-Bravo T. E., et al., 2022, *A&A*, **665**, A123
 Nelder J. A., Mead R., 1965, *The Computer Journal*, **7**, 308
 Nicolas N., et al., 2021, *A&A*, **649**, A74
 Norris J. P., Nemiroff R. J., Scargle J. D., Kouveliotou C., Fishman G. J., Meegan C. A., Paciesas W. S., Bonnell J. T., 1994, *ApJ*, **424**, 540
 Phillips M. M., 1993, *ApJ*, **413**, L105
 Phillips M. M., Lira P., Suntzeff N. B., Schommer R. A., Hamuy M., Maza J., 1999, *AJ*, **118**, 1766
 Piran T., 1992, *ApJ*, **389**, L45
 Ruiter A. J., 2019, *Proceedings of the International Astronomical Union*, **15**, 1–15
 Rust B. W., 1974, PhD thesis, Oak Ridge National Laboratory, Tennessee
 Sanchez et al. B., 2024, in prep
 Scolnic D., et al., 2023, *ApJ*, **954**, L31
 Smith M., et al., 2020, *AJ*, **160**, 267
 Takanashi N., Doi M., Yasuda N., 2008, *MNRAS*, **389**, 1577
 Tripp R., 1998, *A&A*, **331**, 815
 Vincenzi M., et al., 2024, arXiv e-prints, p. arXiv:2401.02945
 Virtanen P., et al., 2020, *Nature Methods*, **17**, 261
 Wang L., Goldhaber G., Aldering G., Perlmutter S., 2003, *ApJ*, **590**, 944
 Wilson O. C., 1939, *ApJ*, **90**, 634
- Zwicky F., 1929, *Proceedings of the National Academy of Sciences*, **15**, 773
 pandas development team T., 2023, pandas-dev/pandas: Pandas, doi:[10.5281/zenodo.8364959](https://doi.org/10.5281/zenodo.8364959), <https://doi.org/10.5281/zenodo.8364959>

APPENDIX A: STRETCH DRIFT WITH REDSHIFT

There is evidence that the stretch distribution of SNe evolves with redshift, as the fraction of older and younger progenitors evolves. [Nicolas et al. \(2021\)](#) give the following relation for the evolution of the SN stretch distribution,

$$P(x_1) = \delta(z)\mathcal{N}(\mu_1, \sigma_1^2) + (1-\delta(z))\left(a\mathcal{N}(\mu_1, \sigma_1^2) + (1-a)\mathcal{N}(\mu_2, \sigma_2^2)\right), \quad (\text{A1})$$

where $\mathcal{N}(\mu, \sigma^2)$ is a normal distribution with mean μ and variance σ^2 and the values of the parameters were $(a, \mu_1, \mu_2, \sigma_1, \sigma_2, K) = (0.51, 0.37, -1.22, 0.61, 0.56, 0.87)$; and the fraction of young supernovae in the population is given by,

$$\delta(z) = \left(K^{-1}(1+z)^{-2.8} + 1\right)^{-1}. \quad (\text{A2})$$

The distribution given by equation (A1) is shown in the upper panel of Fig. A1 for several redshifts, where the vertical dashed lines show the resulting change in the mean x_1 . The relationship between x_1 and the stretch of the supernova is given by ([Guy et al. 2007](#)),

$$s = 0.98 + 0.091x_1 + 0.003x_1^2 - 0.00075x_1^3 \quad (\text{A3})$$

and this is shown in the lower panel of Fig. A1.

Since light curve width is directly proportional to stretch, that means that light curves at redshift $z = 1$ should be approximately 3% wider than those at $z = 0$. This is therefore substantially sub-dominant to the factor of 2 widening expected from time-dilation over the same range.

Compounding this effect, supernovae with wider light curves tend to be brighter, so selection effects might also cause you to find a shift to wider light curves at higher redshifts.

Nevertheless, in the DES-SN5YR data there is no indication that the mean stretch parameter x_1 changes with redshift, see Fig. A2.

Despite the consistency of x_1 in the DES sample we want to quantify how large the *potential* drift in the light curve widths could be if equation (A1) holds. Thankfully this over-estimation can be readily quantified. When you make a mock data set with this intrinsic widening included you find you would actually get a line of $\Delta t \approx 1.03(1+z) - 0.05$ (see Fig. A3). In other words, it would change the slope by ~3%. This is in contrast to the recovered linear model fit in the Fig. 8 caption, hence indicating that this redshift-dependent stretch is not evident in the DES-SN5YR data.

The impact of high-redshift supernovae tending to have a few percent wider stretch than their low-redshift counterparts would cause us to slightly overestimate b . The magnitude of the impact on b depends on your redshift distribution, we estimate a shift of $|\Delta b| \lesssim 0.01$ for the DES data, and we consider this a likely upper limit to the systematic uncertainty on our result. Since our aim in this paper is to fit the light curves with the minimal modelling assumptions (and since we do not see an x_1 trend in our light curve fits) we have chosen *not* to correct for this trend. Instead we note that any potential effect would only be a small deviation around the slope of $w/(1+z) \sim 1$ that we see.

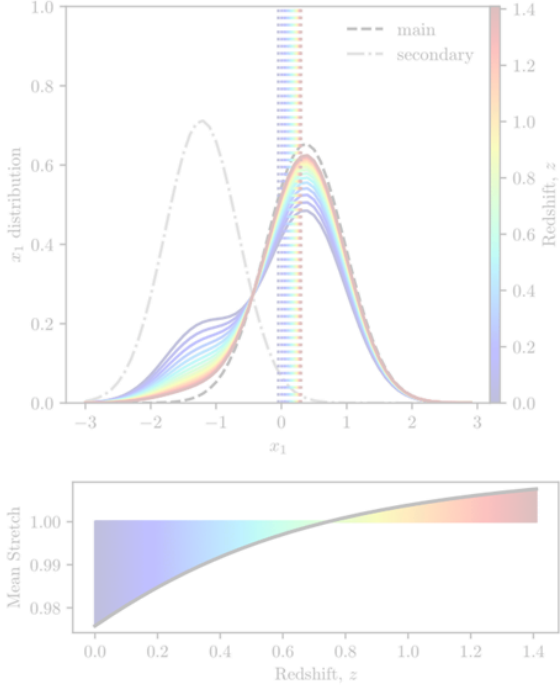


Figure A1. Upper panel: Distribution of x_1 values predicted by Nicolas et al. (2021). The grey and black dashed Gaussians show the two components of the supernova population. The coloured lines show the total distribution for several different redshifts. The vertical dashed lines show the mean of the redshift distribution (in the same colours as the legend). One can see that the mean drifts from low to high x_1 as redshift increases. Lower panel: The black line shows the evolution of the mean stretch (s) of the supernova population with redshift, where colours match the redshifts in the upper legend. The intrinsic light curve width is proportional to s , and therefore light curves are expected to be about 3% wider at $z = 1$ than at $z = 0$. This is much less than the factor of two widening due to time dilation.

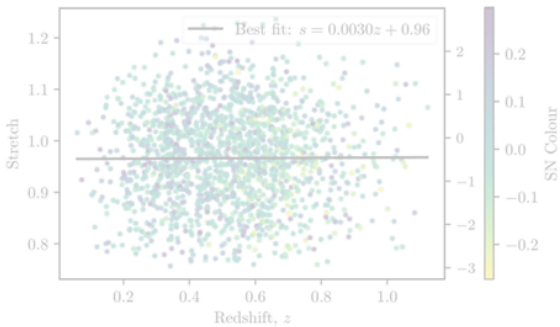


Figure A2. The distribution of stretch in the DES-SN5YR data as a function of redshift (calculated from the SALT3 fitted x_1 values using equation A2), with x_1 shown on the right axis. Fitting a straight line to this distribution shows no significant trend in the stretch with redshift.

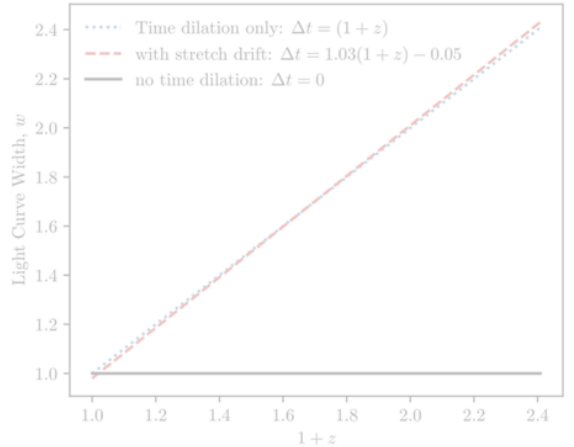


Figure A3. The effect of adding the predicted stretch evolution of SNe Ia vs redshift is to cause the width vs redshift plot to be slightly steeper. If this result is present we therefore expect to slightly overestimate b , as we will attribute that widening to time dilation.

APPENDIX B: REFERENCE CURVE SELECTION DERIVATION

We begin with the definition of redshift,

$$1+z = \frac{\lambda_o}{\lambda_e} \quad (B1)$$

where z is the source redshift, λ_o is the observed wavelength of light and λ_e is the original emission wavelength of light. If we are sampling from a band with central wavelength λ_f during reference curve construction, we need to find a central redshift z_r for our reference SNe selection, given that we are fitting the target light curve in a band of central wavelength λ_f . The idea is to match the original emitted wavelengths and so we can divide by another instance of equation (B1),

$$\frac{1+z}{1+z_r} = \frac{\lambda_f/\lambda_e}{\lambda_r/\lambda_e} = \frac{\lambda_f}{\lambda_r} \quad (B2)$$

Then, we can rearrange to find an expression for our target redshift z_r ,

$$\lambda_r(1+z) = \lambda_f(1+z_r) \quad (B3)$$

$$z_r = \frac{\lambda_r(1+z)}{\lambda_f} - 1 \quad (B4)$$

We can then append a term $\pm\Delta z$ on equation (B4) to give us a range of applicable redshift values as in Section 4.1. Finally, it is useful in the broader context of the paper (and Fig. 3) to show this redshift range in terms of some fraction of the band FWHM of the band that the target SN was observed in, $\delta\Delta\lambda_f$. To do this we set $\Delta z = \delta\Delta\lambda_f/\lambda_f$ and shift the term into the fraction within equation (B4),

$$z_r = \frac{\lambda_r(1+z) \pm \delta\Delta\lambda_f}{\lambda_f} - 1 \quad (B5)$$

which yields the redshift sampling range of equation (3) that we use in the analysis.

APPENDIX C: NULL TEST — NO DE-REDSHIFTING OF REFERENCE LIGHT CURVES

To confirm that our method is able to rule out no time dilation we repeated the analysis without de-redshifting the reference curves. That means that the reference curves would look like the top panel of Fig. 4. If the data were not time dilated, then we should fit consistently $b = 0$ in this case. Fig. C1 clearly shows that this null test fails. Because time-dilation is present in the data, it means that the reference curves are now wider than they should be — making the measured light curve widths narrower. Despite this, the trend for higher-redshift light curves to be wider persists, in very strong contradiction to the no-time-dilation hypothesis.

AFFILIATIONS

- ¹ School of Mathematics and Physics, The University of Queensland, QLD 4072, Australia
- ² Sydney Institute for Astronomy, School of Physics, A28, The University of Sydney, NSW 2006, Australia
- ³ Centre for Gravitational Astrophysics, College of Science, The Australian National University, ACT 2601, Australia
- ⁴ The Research School of Astronomy and Astrophysics, Australian National University, ACT 2601, Australia
- ⁵ Department of Physics & Astronomy, University College London, Gower Street, London, WC1E 6BT, UK
- ⁶ Cerro Tololo Inter-American Observatory, NSF's National Optical-Infrared Astronomy Research Laboratory, Casilla 603, La Serena, Chile
- ⁷ Laboratório Interinstitucional de e-Astronomia - LIneA, Rua Gal. José Cristina 77, Rio de Janeiro, RJ - 20921-400, Brazil
- ⁸ Fermi National Accelerator Laboratory, P. O. Box 500, Batavia, IL 60510, USA
- ⁹ Department of Physics, University of Michigan, Ann Arbor, MI 48109, USA
- ¹⁰ Departamento de Física Teórica and Instituto de Física de Partículas y del Cosmos (IPARCOS-UCM), Universidad Complutense de Madrid, 28040 Madrid, Spain
- ¹¹ Institute of Cosmology and Gravitation, University of Portsmouth, Portsmouth, PO1 3FX, UK
- ¹² University Observatory, Faculty of Physics, Ludwig-Maximilians-Universität, Scheinerstr. 1, 81679 Munich, Germany
- ¹³ Center for Astrophysics | Harvard & Smithsonian, 60 Garden Street, Cambridge, MA 02138, USA
- ¹⁴ Department of Astronomy and Astrophysics, University of Chicago, Chicago, IL 60637, USA
- ¹⁵ Kavli Institute for Particle Astrophysics & Cosmology, P. O. Box 2450, Stanford University, Stanford, CA 94305, USA
- ¹⁶ SLAC National Accelerator Laboratory, Menlo Park, CA 94025, USA
- ¹⁷ Instituto de Astrofísica de Canarias, E-38205 La Laguna, Tenerife, Spain
- ¹⁸ INAF-Osservatorio Astronomico di Trieste, via G. B. Tiepolo 11, I-34143 Trieste, Italy
- ¹⁹ Institut de Física d'Altes Energies (IFAE), The Barcelona Institute of Science and Technology, Campus UAB, 08193 Bellaterra (Barcelona) Spain
- ²⁰ Hamburger Sternwarte, Universität Hamburg, Gojenbergsweg 112, 21029 Hamburg, Germany
- ²¹ Centro de Investigaciones Energéticas, Medioambientales y Tecnológicas (CIEMAT), Madrid, Spain
- ²² Department of Physics, IIT Hyderabad, Kandi, Telangana 502285, India
- ²³ Jet Propulsion Laboratory, California Institute of Technology, 4800 Oak Grove Dr., Pasadena, CA 91109, USA
- ²⁴ Institute of Theoretical Astrophysics, University of Oslo, P.O. Box 1029 Blindern, NO-0315 Oslo, Norway
- ²⁵ Kavli Institute for Cosmological Physics, University of Chicago, Chicago, IL 60637, USA
- ²⁶ Instituto de Física Teórica UAM/CSIC, Universidad Autónoma de Madrid, 28049 Madrid, Spain
- ²⁷ Institut d'Estudis Espacials de Catalunya (IEEC), 08034 Barcelona, Spain
- ²⁸ Institute of Space Sciences (ICE, CSIC), Campus UAB, Carrer de Can Magrans, s/n, 08193 Barcelona, Spain
- ²⁹ Centre for Astrophysics & Supercomputing, Swinburne University of Technology, Victoria 3122, Australia
- ³⁰ Center for Astrophysical Surveys, National Center for Supercomputing Applications, 1205 West Clark St., Urbana, IL 61801, USA
- ³¹ Department of Astronomy, University of Illinois at Urbana-Champaign, 1002 W. Green Street, Urbana, IL 61801, USA
- ³² Santa Cruz Institute for Particle Physics, Santa Cruz, CA 95064, USA
- ³³ Center for Cosmology and Astro-Particle Physics, The Ohio State University, Columbus, OH 43210, USA
- ³⁴ Department of Physics, The Ohio State University, Columbus, OH 43210, USA
- ³⁵ Australian Astronomical Optics, Macquarie University, North Ryde, NSW 2113, Australia
- ³⁶ Lowell Observatory, 1400 Mars Hill Rd, Flagstaff, AZ 86001, USA
- ³⁷ Department of Physics and Astronomy, University of Pennsylvania, Philadelphia, PA 19104, USA
- ³⁸ Departamento de Física Matemática, Instituto de Física, Universidade de São Paulo, CP 66318, São Paulo, SP, 05314-970, Brazil
- ³⁹ George P. and Cynthia Woods Mitchell Institute for Fundamental Physics and Astronomy, and Department of Physics and Astronomy, Texas A&M University, College Station, TX 77843, USA
- ⁴⁰ LPSC Grenoble - 53, Avenue des Martyrs 38026 Grenoble, France
- ⁴¹ Institució Catalana de Recerca i Estudis Avançats, E-08010 Barcelona, Spain
- ⁴² Department of Astrophysical Sciences, Princeton University, Peyton Hall, Princeton, NJ 08544, USA
- ⁴³ Observatório Nacional, Rua Gal. José Cristina 77, Rio de Janeiro, RJ - 20921-400, Brazil
- ⁴⁴ Department of Physics, Carnegie Mellon University, Pittsburgh, Pennsylvania 15312, USA
- ⁴⁵ Department of Physics and Astronomy, Pevenssey Building, University of Sussex, Brighton, BN1 9QH, UK
- ⁴⁶ School of Physics and Astronomy, University of Southampton, Southampton, SO17 1BJ, UK
- ⁴⁷ Computer Science and Mathematics Division, Oak Ridge National Laboratory, Oak Ridge, TN 37831
- ⁴⁸ Department of Physics, Duke University Durham, NC 27708, USA
- ⁴⁹ Université Grenoble Alpes, CNRS, LPSC-IN2P3, 38000 Grenoble, France
- ⁵⁰ Department of Astronomy, University of California, Berkeley, 501 Campbell Hall, Berkeley, CA 94720, USA
- ⁵¹ Lawrence Berkeley National Laboratory, 1 Cyclotron Road, Berkeley, CA 94720, USA

This paper has been typeset from a TeX/LaTeX file prepared by the author.

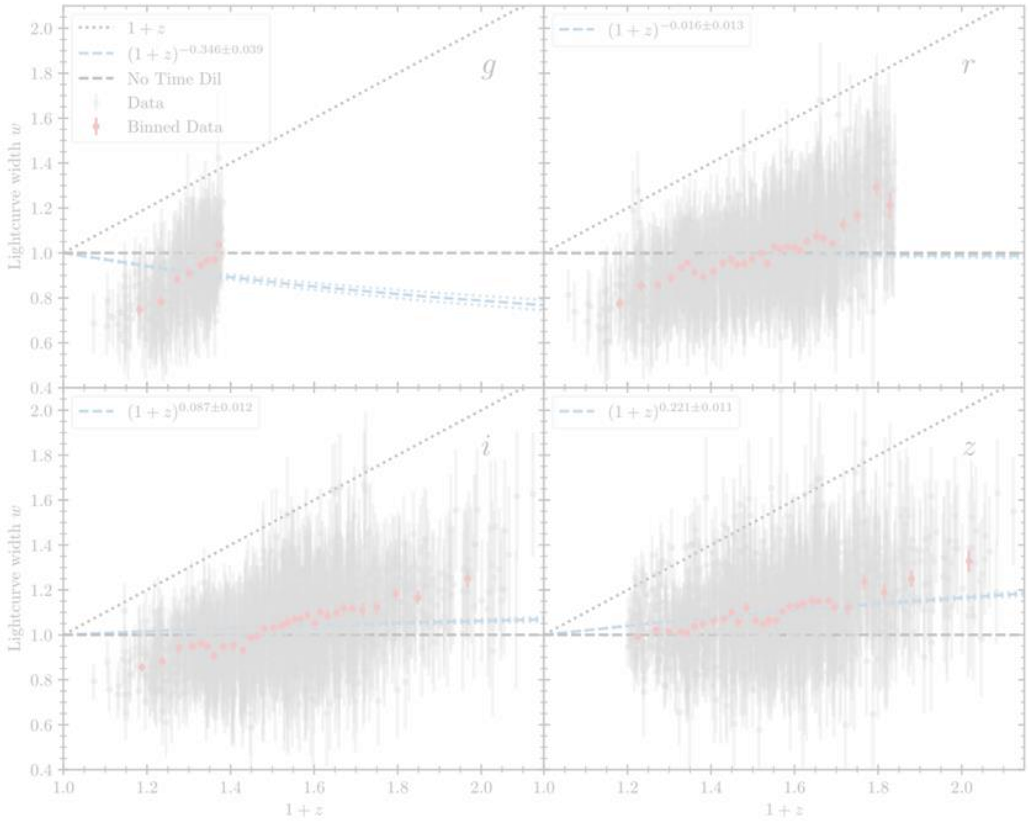


Figure C1. Light curve widths measured with respect to a reference curve that has *not* been de-time-dilated. We nevertheless still see a persistent trend of increasing light curve width with redshift. The vertical offset from the $(1+z)$ line arises because the non-de-time-dilated reference curves are wider than rest-frame light curves, i.e. this offset is yet another indication of time dilation. The black horizontal dashed line indicates no time dilation and the blue dashed lines are (poor) $(1+z)^b$ model fits to the data. If there was no time dilation, these fits would be horizontal lines with $b = 0$.